Experimental Neurology **172,** 363–376 (2001)
doi:10.1006/exnr.2001.7823, available online at http://www.idealibrary.com on IDEAL®

# Parkinsonian Motor Deficits Are Reflected by Proportional A9/A10 Dopamine Neuron Degeneration in the Rat

A. E. Moore,* F. Cicchetti,* J. Hennen,† and O. Isacson*,[1]

*Neuroregeneration Laboratory, Harvard Medical School/McLean Hospital, Belmont, Massachusetts 02478; and †Department of Biostatistics, McLean Hospital, Belmont, Massachusetts 02478

Received August 22, 2001; accepted September 20, 2001

**In a model of Parkinson's disease (PD), amphetamine, a dopamine (DA)-releasing drug, fails to induce ipsilateral drug rotations in a proportion of rats with complete unilateral 6-hydroxydopamine (6-OHDA) lesions of the medial forebrain bundle and DA neurons of the substantia nigra. To investigate this phenomenon, individual 6-OHDA lesions (measured by tyrosine hydroxylase immunohistochemistry) in the substantia nigra pars compacta (A9), ventral tegmental area (A10), and striatum were examined in conjunction with outcomes of four behavioral tests. The behavioral tests were skilled paw reaching, a head-turning test, and apomorphine (0.05 mg/kg) and amphetamine (4 mg/kg) drug-induced rotations. Four weeks postlesion, ipsilateral side bias measured by the head-turning test correlated strongly with extent of A9 DA neuronal lesion. Additional A10 neuronal DA lesions did not substantially improve the model fit, indicating that the head-turning bias was primarily A9 dependent. In contrast, total head-turning activity increased monotonically with lesions of A10 striatal DA fibers. Skilled paw-reaching accuracy decreased with increased lesion of both A9 and A10 DA neuronal systems. Associating amphetamine-induced rotations with extent of A9 DA lesion generated a second-order polynomial model, $y = -11.1x + 0.20x^2 + 208.7$ ($R^2 = 0.73$), with an overall $F$ ratio (df = 2,21) of 28.4 ($P < 0.0001$). This model predicts that an A9 DA lesion of about 50% is required to induce an ipsilateral turning bias, after which rotations increase with the degree of A9 DA neuronal lesion. No further change in rotational behavior was seen until an additional A10 DA lesion reached 60%, after which the rotational response decreased. This analysis provides tests that differentiate between A9 DA degeneration and combined A9/A10 lesions in animal models and in addition allows predictive testing of PD therapeutic intervention at a preclinical level.** 

[1] To whom correspondence and reprint requests should be addressed at 115 Mill Street, McLean Hospital/Harvard Medical School, Belmont, MA 02478. Fax: (617) 855-3284. E-mail: isacson@helix.mgh.harvard.edu.

*Key Words:* **motor behavior; drug effects/pharmacology; 6-hydroxydopamine; substantia nigra; ventral tegmental area; nucleus accumbens; striatum; rat; amphetamine; apomorphine.**

## INTRODUCTION

Investigation of therapeutic strategies for Parkinson's disease (PD), specifically the substantia nigra and DA function within the midbrain, was substantially aided by Ungerstedt and colleagues' development of the 6-hydroxydopamine (6-OHDA) rat model (43, 46). In this procedure, DA neurons are selectively destroyed by infusion of the neurotoxin 6-OHDA into the medial forebrain bundle (mfb). Neuron extinction is achieved by active uptake of 6-OHDA through the DA transporter exclusive to DA neurons (6, 18). The procedure is designed to target the DA neurons of the substantia nigra pars compacta (SNc, also known as the A9 nucleus) that degenerate in PD. However, DA neurons more medial to the A9, making up the ventral tegmental area (VTA, or A10), are often included in these lesions (9, 44). The nigrostriatal tract connects the DA cells of the A9 to the dorsolateral striatum (DL striatum), while the mesolimbic part of the tract connects the neurons of the A10 to the ventro medial (VMe) striatum, nucleus accumbens (NAC), olfactory tubercle, and layer VI of the neocortex (52).

Unilateral mfb lesion causes manifestation of motor asymmetry to low doses of DA agonists (2, 49), as a result of an upregulation of DA receptors in the lesioned striatum (8, 45). In untreated PD patients, studies utilizing PET DA ligand or postmortem autoradiographic technology have demonstrated this upregulation to be localized within the DA $D_2$ receptor population (39). These studies suggest that $D_2$ receptor binding constants increase in PD patients by approximately 45%.

Unilateral motor deficits caused by unilateral 6-OHDA A9 lesions are not easily detectable in the rat, unless drugs acting on DA neurons or receptors accen-



0014-4886/01 $35.00

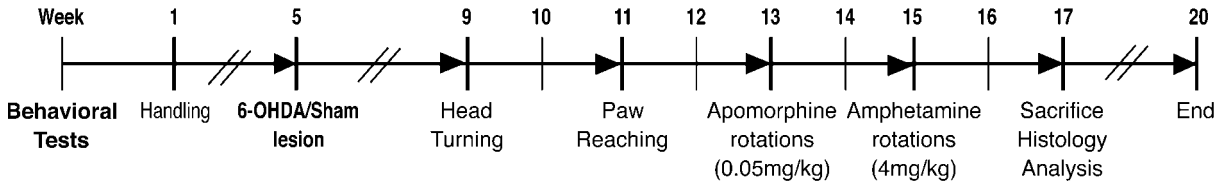


**FIG. 1.** Experimental time line depicting the order in which all behavioral tests were carried out. Thirty-two rats with a range of either A9 dopamine (DA) or A9 plus A10 DA lesions completed four behavioral tests over a 20-week period. Lesions were made by infusion of either two doses of 6-OHDA (27.5 or 46 $\mu$g) or saline (week 5). Rats underwent head-turning tests at 4 weeks postlesion (week 9). Paw-reaching accommodation took place 6 weeks postlesion and testing at 7 weeks postlesion (weeks 11 and 12). Apomorphine rotations (0.05 mg/kg) were induced at 8 weeks postlesion (week 13) and amphetamine rotations (4 mg/kg) were induced at 10 weeks postlesion (week 15). All animals were sacrificed at 12 weeks postlesion. Note that testing was carried out in the order shown to minimize the effects of amphetamine and apomorphine administration on spontaneous behavioral responses.

tuate a side bias that can be measured (48). The mesolimbic DA system's role in behavioral responses to apomorphine and amphetamine is not yet fully understood (10, 26, 27). Drug-induced and spontaneous tests of rats with 6-OHDA lesions suggest that lesions of A10 DA cells cause an increase in the response to apomorphine, reduction of amphetamine-induced motor activation, and disruption of feeding and hoarding behavior (14, 22, 25, 28, 29, 41). Histological analysis of 6-OHDA-lesioned rats has revealed the paradox that not all well-lesioned rats rotate (27, 35, 44). We believe that, when evaluating the 6-OHDA rat model as a tool for investigation of potential therapies for motor deficits in PD, it is important to determine the contribution of additional A10 DA cell loss to characteristic behavioral responses in the A9 DA lesioned rat. It is also important to examine the effects of these individual cell groups on spontaneous and skilled motor activity. Here we report several experiments correlating the extent of A9 and A10 DA lesion with both apomorphine- and amphetamine-induced rotations with the results of two spontaneous behavioral tests: skilled paw reaching and a modified version of a head-turning test. These experiments involved a large series of rats with varying degrees of A9 plus A10 6-OHDA or sham lesions by saline infusions. By these analyses, we established correlates of behavior with the extent and specificity of lesion, thus permitting extensive analysis of subsequent treatment paradigms. These results also led to the formulation of two testable hypotheses (H) of functional effects of the A9 and A10 cell groups when considering both drug-induced and spontaneous motor behavior: H1, DA neurons of the A9 affect side bias; H2, neurons of the A10 have an amplification effect on the A9 response to lesion and, after a certain threshold is reached, result in a dampening of the side bias response.

## METHODOLOGY

We used seven behavioral measurements to assess ipsilateral side bias: apomorphine-induced rotations, amphetamine-induced rotations, head-turning ipsilateral side bias, head-turning total activity, skilled paw reaching (left paw and right paw), and total amount eaten with the left paw during the paw-reaching tests.

We hypothesize (H1) that these seven behavioral variables are associated with the extent (%) of A9 lesion in a manner approximated by a $\int$-shaped curve. That is, at low levels of A9 lesion, there is limited or even zero behavioral response, up to a certain threshold level of A9 lesion, beyond which there is a steep gradient in the side-bias measures. We further hypothesize (H2) that A10 lesions enhance the side-bias response up to a certain threshold, beyond which there is a dampening of the side-bias measures.

The interventions used to examine these hypotheses were 6-OHDA lesions of A9 and A9 plus A10 DA neurons, with intensity at several levels over the entire range (0–100%) of the A9–A10 DA lesion extent.

### *Summary of Experiments*

With the aim of producing a population of rats with variable DA lesions, 32 female (300 g) Sprague–Dawley rats (Charles River) were lesioned. Two groups of 16 rats, separated by 1 week, received stereotaxic infusion of either saline or one of two different doses of 6-OHDA (46 or 27.5 $\mu$g). Each rat underwent four behavioral tests: head turning, D-amphetamine-induced rotations, apomorphine-induced rotations, and skilled paw reaching. These tests were carried out in a sequence that prevented drug administration from affecting spontaneous behavioral testing (Fig. 1). Rats were kept at room temperature on a 12-h dark/light cycle. Four rats occupied one home cage and had unlimited access to water and food pellets. All necessary steps were taken to ensure the health of the animals, which were maintained to the standard specified by the Institutional Animal Care and Use Committees and Harvard Medical Area Standing Committee on Animals.

### *6-OHDA Lesions*

Rats ($n$ = 16) received mfb and substantia nigra infusions of 0.9% saline + 0.01% ascorbic acid using Kopf instrument stereotactic frames; $n$ = 8 received an effective dose of 46 $\mu$g 6-OHDA in 0.9% saline + 0.01%

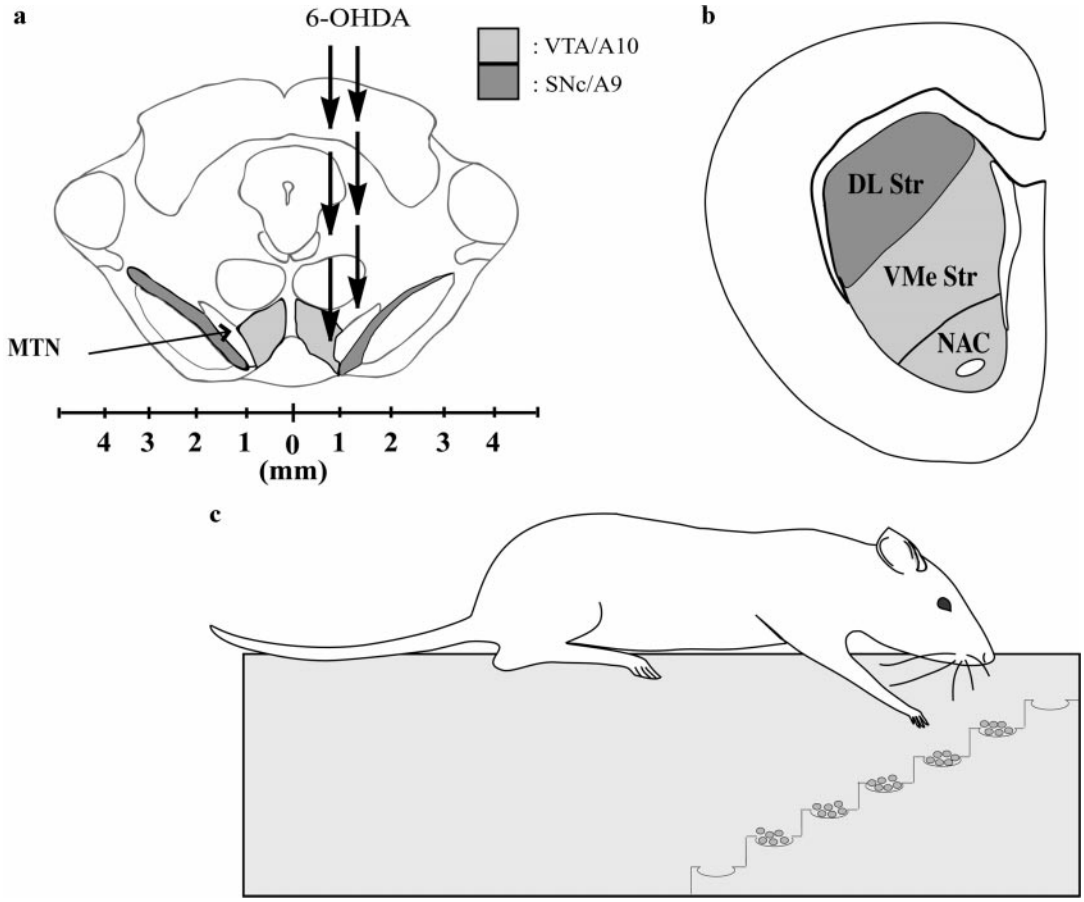


**FIG. 2.** (a) Schematic drawing depicting a frontal section of the rat brain at the level of the SN/VTA showing the variation in lateral placement of the 6-OHDA lesion. This drawing also outlines the anatomical borders of the SNc and VTA nuclei which were used to perform the $TH^+$ cell counts in this study. $TH^+$ neurons found lateral to the MTN were defined as being in the SNc, while those medial to this tract were defined as VTA neurons. (b) Schematic drawing of a frontal section of the rat's left striatum depicting the subdivision of the striatum used for this study: the dorsolateral (DL) striatum and the ventromedial (VMe)/nucleus accumbens (NAC) striatum. (c) Schematic drawing of the paw-reaching apparatus which consists of a plexiform glass container with a platform. A six-step staircase is located on either side of the platform and each step has a well in which six food pellets are placed. Steps 2–5 are baited and rats, maintained at 80% of their free-feeding weight, reach for food pellets during a 20-min test carried out over 10 consecutive days. Total numbers of pellets eaten and taken are recorded separately. Each rat's accuracy is determined as a function of the number of pellets eaten divided by the number of pellets taken.

ascorbic acid, while the remaining 8 rats received infusion of 27.5 $\mu$g 6-OHDA in 0.9% saline + 0.01% ascorbic acid. Infusions were made using a 10-$\mu$l Hamilton microsyringe, fitted with a 22-gauge beveled (45°) Hamilton needle, into two sites from Bregma: site 1, AP −4.4, ML −1.3, DV −7.8, and incisor bar (IB) −2.4; site 2, AP −4.0, ML −0.9, DV −8.0, and IB +3.4 (Fig. 2a). The solutions were kept on ice (4°C) and protected from exposure to light to minimize oxidation. Volumes of 3.0 $\mu$l were injected into site 1 and 2.5-$\mu$l volumes were injected into site 2, with an infusion rate of 1 $\mu$l/min. After the total dose was administered at each site, the needle was allowed to remain in the brain for 3 min.

### *Behavioral Studies*

*Rotational behavior.* Rotational behavior was assessed using a modified version of the method developed by Ungerstedt (49). Apomorphine rotations (0.05 mg/kg) were induced at 8 weeks postlesion (40-min test duration); amphetamine-induced rotations (4 mg/kg) were monitored during a 90-min test at 10 weeks postlesion (Fig. 1). A harness consisting of two elastic bands was placed around the chest of the rat, behind both elbows. The rat was placed in a spherical bowl and the harness was attached by a Velcro fitting, to steel wire approximately 12 inches long, in turn fitted to a rotometer determining the direction in which the rat turns. The net rotational asymmetry score was expressed as full body turns per minute (16).

*Skilled paw reaching.* Skilled forelimb paw-reaching ability was assessed at 7 weeks postlesion via a modified version of the "staircase test" developed by Montoya *et al.* (34). The paw-reaching apparatus consists of a plexiform glass container with two compartments. The platform, onto which the rat is placed, has

a 70-mm trough on both sides, in which a seven-step staircase is located (Fig. 2c). Starting 6 weeks postlesion, rats were maintained at 80% of their free-feeding body weight, as described by Montoya *et al.* (34) and Garcia *et al.* (17). In the first 2 days of testing, the rats were habituated to the test boxes by placing them in the empty container for 20 min per day. During habituation, the rats had free access to water, but no food. Starting at day 3, paw-reaching tests were carried out for 10 consecutive days. The rats were placed in the cage with steps 2–6 of the apparatus baited with 6 × 45-mg food pellets per step, with a total of 30 food pellets per side. Each rat was weighed daily to ensure body weight remained at about 80% of the free-feeding weight. The tests were run over a duration of 20 min. The accuracy measure was calculated as the total number of pellets eaten by the left paw divided by the total number of pellets taken by the left paw. These ratios were averaged for the last 3 days of testing, yielding an average accuracy score for each rat.

*Head turning.* In this test, modified from Henderson *et al.* (20), the rat's head position relative to the body was measured at 4 weeks postlesion (Fig. 1). In these tests, the animals were brought into a quiet room with dim lighting and allowed to habituate for 2 min. One rat was put into each of five observation cages, placed on the floor for easy viewing of the rats' movements, and given an additional 2 min to habituate to these cages. Then, the number of head turns made every second for 3 × 1-min tests per rat was recorded to the beat of a digital metronome. A deviation greater than $10^0$ was considered to be a "head turn." A judgment of the position of the head was made regardless of the rat's activity, including rearing and grooming. Left and right turns were recorded separately, and the total number of turns made in the 3-min sessions was calculated per rat. The net number of seconds (counts were made every second) the head was positioned both ipsilaterally and contralaterally was recorded. From this, ipsilateral side bias and overall head-turning activity indices were calculated.

### *Tyrosine Hydroxylase Immunohistochemistry*

Animals were deeply anesthetized with sodium pentobarbital (300 mg/kg, i.p.) and perfused intracardially with 100 ml heparinized saline followed by 200 ml 4% paraformaldehyde (PFA) in 0.1 M PBS, pH ~ 7.4. The brains were removed, postfixed in 4% PFA for 6–8 h, and equilibrated in 20% sucrose in 0.1 M PBS for cryoprotection and six series of coronal sections were cut at 40-$\mu$m thickness on a freezing microtome. Two series were processed for free-floating TH immunohistochemistry. After 3 × 10-min rinses in 0.1 M phosphate-buffered saline (PBS), endogenous peroxidase activity was quenched by rinsing in 3% $H_2O_2$ for 30 min. After a further three rinses in PBS, sections were preincubated with 2% normal bovine serum (NBS) and 0.1% Triton X-100, in PBS for 30 min, then transferred into an incubation medium of primary anti-TH raised in rabbit (dilution 1:200, PelFreeze Biologicals, Inc., MA), 2% NBS, 0.1% Triton X-100 in PBS, incubated overnight at 4°C. Sections were rinsed three times for 10 min each in PBS and incubated for 60 min at room temperature in an incubation medium of biotinylated goat anti-rabbit IgG (dilution 1:200), 2% NBS, 0.1% Triton X-100 in PBS. After three rinses in PBS, the sections were transferred to a Vectastain ABC Elite solution in PBS for 90 min. Following two washes in PBS, and one in TBS, the sections were developed in a solution of 3,3′-diaminobenzidine (Sigma, 0.05%, in TBS with 0.01% $H_2O_2$) serving as chromagen. Serial sections of two series were placed on gelatin-coated slides, left to dry overnight, dehydrated in ascending alcohol concentrations, cleared in xylene, and then coverslipped.

### *TH Cell Counts*

Cell counts were performed blind. An independent investigator (Ms. Therese Anderson) implemented a code which concealed the identity of all slides while cell counts were made. Slide identities were not revealed until correlations were complete. $TH^+$ cell counts were obtained for every third section through A9 and A10 and were made for both lesioned and unlesioned A9 and A10 separately. A9 was defined as lateral to the medial terminal nucleus of the accessory optic tract (MTN, level AP − 5.3 mm in the atlas of Paxinos and Watson) (38); A10 was medial to this nucleus (Fig. 2a). All cells present were counted under brightfield illumination at 40× magnification. Data were expressed as relative "% lesioned." Abercrombie correction (1) was performed using the average $TH^+$ cell diameter. This was attained by measuring the diameters of 20 $TH^+$ cells from A9 and A10, obtained from both the left and right sides of five rat brains. The mean diameters of the left and right A9 and A10 cells were calculated, and the mean diameters of all cells were determined. Abercrombie correction (1) was then carried out using the two data sets: first by using the mean cell diameter for the separate cell groups and second by using the overall mean. No significant differences were found in the resulting cell counts. Accordingly, the overall mean $TH^+$ cell diameters were used for subsequent correlations and analyses.

### *Densitometry*

Quantifications of the striatal lesion and $TH^+$ innervation were obtained using a Zeiss Axioskop microscope with a Real Time Spot camera (Diagnostic Instruments Inc., MI) and NIH Image 1.41 (NIH) as previously described (11–13). Optical density measurements of $TH^+$ innervation were taken from the areas of the striatum to which A9 and A10 project. These were measured separately for the lesioned and unlesioned sides. A9 was defined as projecting to the DL striatum;

A10 was defined as projecting to the VMe/NAC striatum (Fig. 2b). The areas were outlined in four sections per rat at 200 $\mu$m apart. Measurements were averaged per rat and expressed as relative % lesioned for each of the three areas measured.

### *Statistical Analysis*

Outcome measures included apomorphine-induced rotations in 40 min, amphetamine-induced rotations in 90 min, and number of head turns made in 3 min and paw reaching. Explanatory factors included extent of A9 DA lesion (in %), extent of A10 DA lesion (in %), DL striatal density [optical densitometry (OD) units], and VMe/NAC striatal density (OD units). Distribution properties of the outcome measures and explanatory factors were examined using univariate kernel density estimate methods and scatterplots for bivariate pairings. The strength and patterns of correlations of outcome measures with explanatory factors were assessed by regression modeling methods. For some outcome–explanatory factor pairs, linear regression methods were used. For others, in which scatterplots of the outcome measure–explanatory factor association had the appearance of a flat initial section, extending to a certain threshold, followed by a rapidly increasing section or some other nonlinear association, one of three regression modeling methods was employed: piecewise linear regression, polynomial regression, and semilogarithmic (dependent variable logarithmically transformed) regression.

Heuristically selected modeling equations can provide more realistic representations of rotational behavior (for example, of threshold effect). Therefore, in our analyses, a polynomial or semilogarithmic model was chosen in preference to a linear model to provide a closer data fit (except at the extreme values, near 0 or 100% of the lesioning distribution). In particular, we fit polynomial or semilogarithmic models when scatterplots suggested the threshold effect described above, which obviously cannot be modeled adequately with a linear model.

Outlier observations were identified within each outcome measure–explanatory factor pair, defined as individual rats that were consistent nonperformers in four of the behavioral tests. Nonperformers were identified by response measures three or more standard deviations different from predicted values based on the model best describing the data set. Identified outliers were excluded from subsequent modeling analyses.

For each outcome–explanatory factor pair, the best-fitting regression model was selected from among the three candidate modeling methods named above. This selection was done via a two-step method: by inspection of scatterplots to decide between linear and nonlinear modeling and then by likelihood ratio test for nested models or comparison of model $\chi^2$ statistics for nonnested contrasts. In nonlinear contrasts, when likelihood ratio tests or $\chi^2$ comparisons indicated near-equivalence of contrasted models, we selected the simpler, more parsimonious model in preference to the more complex model. For each outcome measure–explanatory factor pair, after selection of the best-fitting model, the pairwise correlation was depicted graphically, in a scatterplot with included best-fit curve, and numerically, in a summary table (Table 1) showing pairwise regression modeling results. For the semilogarithmic models, the best-fit curve values were adjusted by the variance from the regression because of the logarithmic change-of-variable. Statistical analyses were carried out using the software program Stata (Stata Corp., College Station, TX).

## RESULTS

### *Characterization of Lesions*

Analysis of lesions using OD data confirmed a close approximation to normal distribution of the several outcome and explanatory variables in the study (Fig. 3). $TH^+$ analysis confirmed that a range of lesions between 0 and 100% were obtained. Frontal sections at the level of the SN demonstrating examples of typical lesions found during analysis are shown (Fig. 4).

### *Drug-Induced Behavior*

*Apomorphine-induced rotations.* Among several regression-modeling methods tried with these data, including polynomial regressions of the order 1, 2, or 3 and semilogarithmic regressions, the model best describing the effect of A9 DA lesion ($x$) on apomorphine-induced rotations ($y$) was found to be a semilogarithmic fit: $\ln(y) = 0.051x + 0.221$ ($R^2 = 0.69$). This regression was highly statistically significant with an overall $F$ ratio (df = 1,22) of 55.5 ($P < 0.0001$) (Fig. 5a). The model indicates that contralateral side bias is not apparent until lesions become inclusive of more than 70–80% of SNc DA cells. A clear threshold is seen at this point, after which contralateral rotational behavior intensifies with progressive increase in A9 DA lesion. Similarly, the association between DL striatal $TH^+$ fiber loss and apomorphine-induced rotations followed a strong exponential trend, similar to that observed with the A9 DA lesions. This pattern (Fig. 5b) was statistically significant ($R^2 = 0.19$), with an overall $F$ statistic (df = 1,22) of 5.08 ($P = 0.034$). Figure 5b suggests the existence of a threshold lesion of 70–80%, after which contralateral rotational behavior increases intensely as $TH^+$ fibers are lost. The effect of additional A10 DA lesion ($x$) on apomorphine-induced rotations ($y$) was best described by a semilogarithmic fit: $\ln(y) = 4.60x - 28.7$. This model was statistically significant ($R^2 = 0.55$), with an overall $F$ ratio (df = 1,22) of 33.4 ($P < 0.0001$) (Fig. 5c). These data suggest that contralateral side bias continues to increase with increasing lesion extent until additional lesion of 50–60% of

**TABLE 1**

Summary of Best-Fitting Models

| Interventions ($x$) | Behavioral outcome ($y$) | Best-fitting functional form | $F$ statistic | df | $R^2$ | $P$ |
|---|---|---|---|---|---|---|
| A9 lesion | Apomorphine rotations | $\ln(y) = 0.051x + 0.221$ | 55.5 | 1, 22 | 0.69 | <0.0001 |
| | Amphetamine rotations | $y = 0.20x^2 - 11.1x + 208.7$ | 28.4 | 2, 21 | 0.73 | <0.0001 |
| | Head-turning ipsilateral bias | $y = 0.90x - 24.5$ | 21.9 | 1, 22 | 0.5 | <0.0001 |
| | Head-turning total activity | NS | — | | — | — |
| | Paw reaching (left) | $y = -0.003x^2 - 0.005x + 61.0$ | 3.31 | 2, 19 | 0.26 | 0.05 |
| | Paw reaching (right) | NS | — | | — | — |
| | Paw-reaching total eaten (left) | $y = -0.02x^2 + 1.77x + 53.5$ | 3.95 | 2, 19 | 0.29 | 0.037 |
| TH density DL striatum | Apomorphine rotations | NS | — | | — | — |
| | Amphetamine rotations | $y = 3.27x + 1.32x^2 + 79.3$ | 3.58 | 2, 21 | 0.25 | 0.04 |
| | Head-turning ipsilateral bias | $y = 0.75x - 26.7$ | 7.44 | 1, 22 | 0.25 | <0.012 |
| | Head-turning total activity | NS | — | | — | — |
| | Paw-reaching accuracy (left) | NS | — | | — | — |
| | Paw reaching (right) | NS | — | | — | — |
| | Paw-reaching total eaten (left) | NS | — | | — | — |
| A10 lesion | Apomorphine rotations | $\ln(y) = 4.60x - 28.7$ | 33.4 | 1, 22 | 0.55 | <0.0001 |
| | Amphetamine rotations | $y = -0.008x^3 + 0.77x^2 + 1.32x - 2.40$ | 13.38 | 3, 20 | 0.67 | <0.0001 |
| | Head-turning ipsilateral bias | $y = 0.96x - 8.30$ | 16.3 | 1, 22 | 0.43 | 0.0005 |
| | Head-turning total activity | NS | — | | — | — |
| | Paw reaching (left) | $y = -0.011x^2 + 0.33x + 58.9$ | 10.1 | 2, 19 | 0.51 | <0.001 |
| | Paw reaching (right) | NS | — | | — | — |
| | Paw-reaching total eaten (left) | $y = -0.02x^2 + 0.43x + 82.8$ | 6.53 | 2, 19 | 0.41 | 0.0069 |
| TH density Vme/NAC striatum | Apomorphine rotations | NS | — | | — | — |
| | Amphetamine rotations | NS | — | | — | — |
| | Head-turning ipsilateral bias | NS | — | | — | — |
| | Head-turning total activity | $y = 0.45x + 50.5$ | 4.93 | 1, 22 | 0.18 | <0.037 |
| | Paw reaching (left) | NS | — | | — | — |
| | Paw reaching (right) | NS | — | | — | — |
| | Paw-reaching total eaten (left) | NS | — | | — | — |

*Note.* NS, no significance found.

A10 DA neurons is achieved. Correlation of VMe/NAC striatal density with apomorphine-induced rotations was also statistically significant ($R^2 = 0.18$), with an $F$ ratio (df = 1,22) of 4.95 ($P = 0.037$). However, a strong trend in apomorphine-induced rotation–A10 DA lesion data suggests that a threshold loss of $TH^+$ fibers in the VMe/NAC striatum of 70–80% is required before rotational behavior is observed (Fig. 5d).

*Amphetamine-induced rotations.* The patterns of amphetamine-induced rotations in their associations with lesion showed the same J-shaped curves noted for apomorphine-induced rotations. For A9 DA lesions, a second-order polynomial regression was found to be the best-fitting model correlating extent of lesion with number of amphetamine-induced rotations (Fig. 6a). This model, $y = -11.1x + 0.20x^2 + 208.7$, was strongly statistically significant ($R^2 = 0.73$), with an overall $F$ ratio (df = 2,21) of 28.4 ($P < 0.0001$). The scatterplot (Fig. 6a) suggests that no amphetamine rotations are induced until A9 cell numbers are depleted by about 50%, after which the ipsilateral side bias increases monotonically with extent of lesion. For the association between the extent of DL striatal optical density loss ($x$) and the number of amphetamine-induced rotations ($y$), a second-order model also was found to provide best fit. This quadratic model, $y = 3.27x + 1.32x^2 + 79.3$, was statistically significant ($R^2 = 0.25$), with an overall $F$ ratio (df = 2,21) of 3.58 ($P = 0.04$). The scatterplot (Fig. 6b) suggests that ipsilateral side bias does not appear until a 50% loss in TH density is attained, from which point a progressive monotonic increase in ipsilateral side bias occurs.

A cubic model was found to provide best fit in models correlating the extent of additional A10 DA lesion ($x$) with the number of amphetamine-induced rotations ($y$). This cubic model, $y = 1.32x + 0.77x^2 - 0.008x^3 - 2.40$, was highly statistically significant ($R^2 = 0.67$), with an overall $F$ ratio (df = 3,20) of 13.38 ($P < 0.0001$). The scatterplot (Fig. 6c) suggests that additional A10 DA lesions greater than approximately 20% were associated with substantially increased numbers of amphetamine-induced rotations. An apparent asymptote was reached at approximately 60% DA cell loss, after which additional A10 DA lesion was clearly associated with a dampening effect on the side bias caused by A9 DA lesion.

### *Non-drug-Induced Behavior*

*Head turning.* The extent of ipsilateral side bias measured by head turning ($y$) was positively and linearly correlated with the magnitude of A9 DA lesion

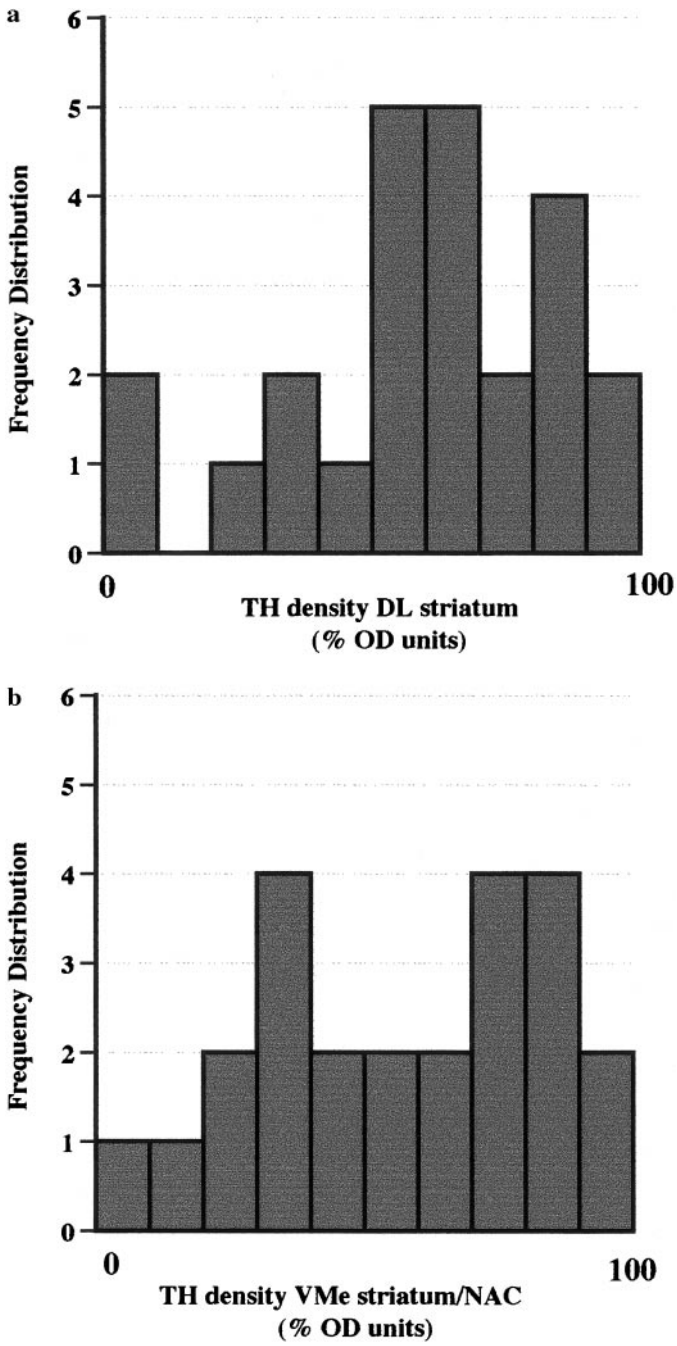


**FIG. 3.** Distributions of $TH^+$ fiber density in the DL striatum and VMe striatum/NAC. Optical density (OD) measurements were made using NIH Image 1.61 and statistical analyses were performed using Stata software (Stata Corp.). (a) Frequency distribution of the percentage loss of $TH^+$ fibers in the right DL striatum compared to the intact side expressed as percentage of relative OD. A close approximation to normal distribution for DL striatal lesions was achieved. (b) Frequency distribution of the percentage loss of $TH^+$ fibers in the right VMe striatum and NAC compared to the intact side expressed as percentage of relative OD. The distribution of lesions in the VMe striatum and NAC was also a close approximation to a normal distribution.

($x$). The best-fitting regression model $y = 0.90x - 24.5$ was strongly statistically significant ($R^2 = 0.50$). This model had an overall $F$ statistic (df = 1,22) of 21.9 ($P <$ 0.0001). Figure 7a suggests that ipsilateral side bias, as measured by the head-turning test, increases linearly throughout the entire measured range (0–100%) of A9 DA lesion. These data are supported by the correlation between optical density of DL striatum and head-turning bias, for which a positive linear correlation was also found. The regression equation was $y = 0.75x - 26.7$, with $R^2 = 0.25$ and with an overall $F$ statistic (df = 1,22) of 7.44 ($P < 0.012$). The scatterplot (Fig. 7b) suggests that ipsilateral side bias as measured by head turning increases linearly throughout the measured range of the lesions.

For the association between ipsilateral side bias and

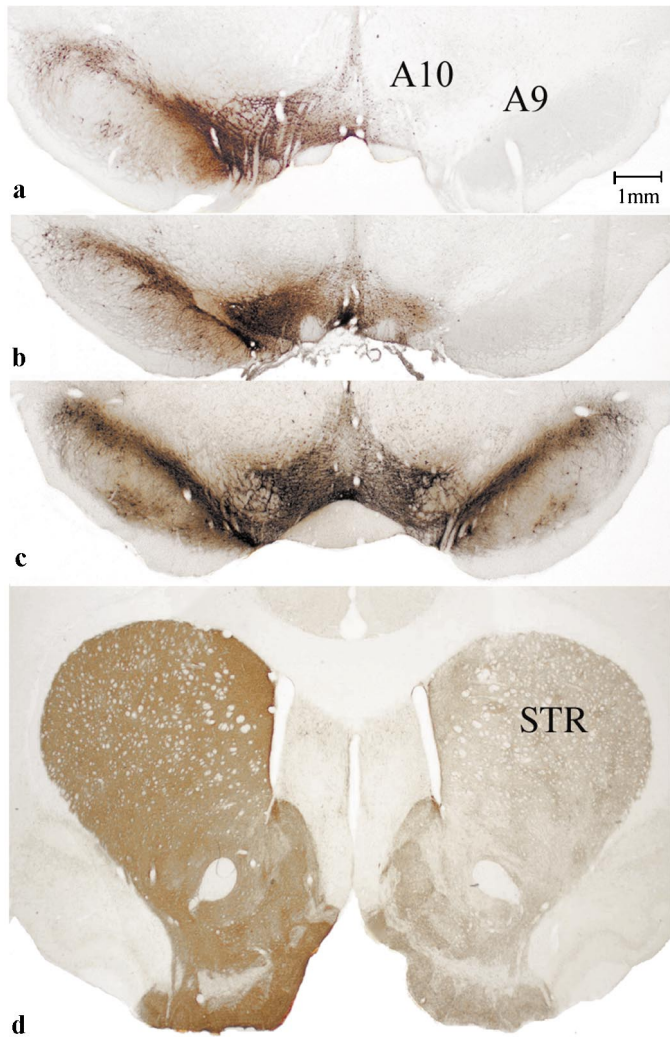


**FIG. 4.** Low-power photomicrographs of rat frontal sections at the level of the SN and striatum illustrating the different types of lesions assessed by TH immunostaining. (a) Photomicrograph illustrating a complete loss of $TH^+$ neurons in the right A9 and A10 nuclei. (b) Example of a complete loss of A9 DA neurons with partial A10 DA loss. (c) Frontal section taken from a rat with a sham lesion, clearly showing absolute sparing of A9 and A10 DA neurons. (d) Photomicrograph illustrating a typical striatal $TH^+$ fiber denervation following a complete A9/A10 6-OHDA lesion. Scale bar represents 1 mm in all figures.

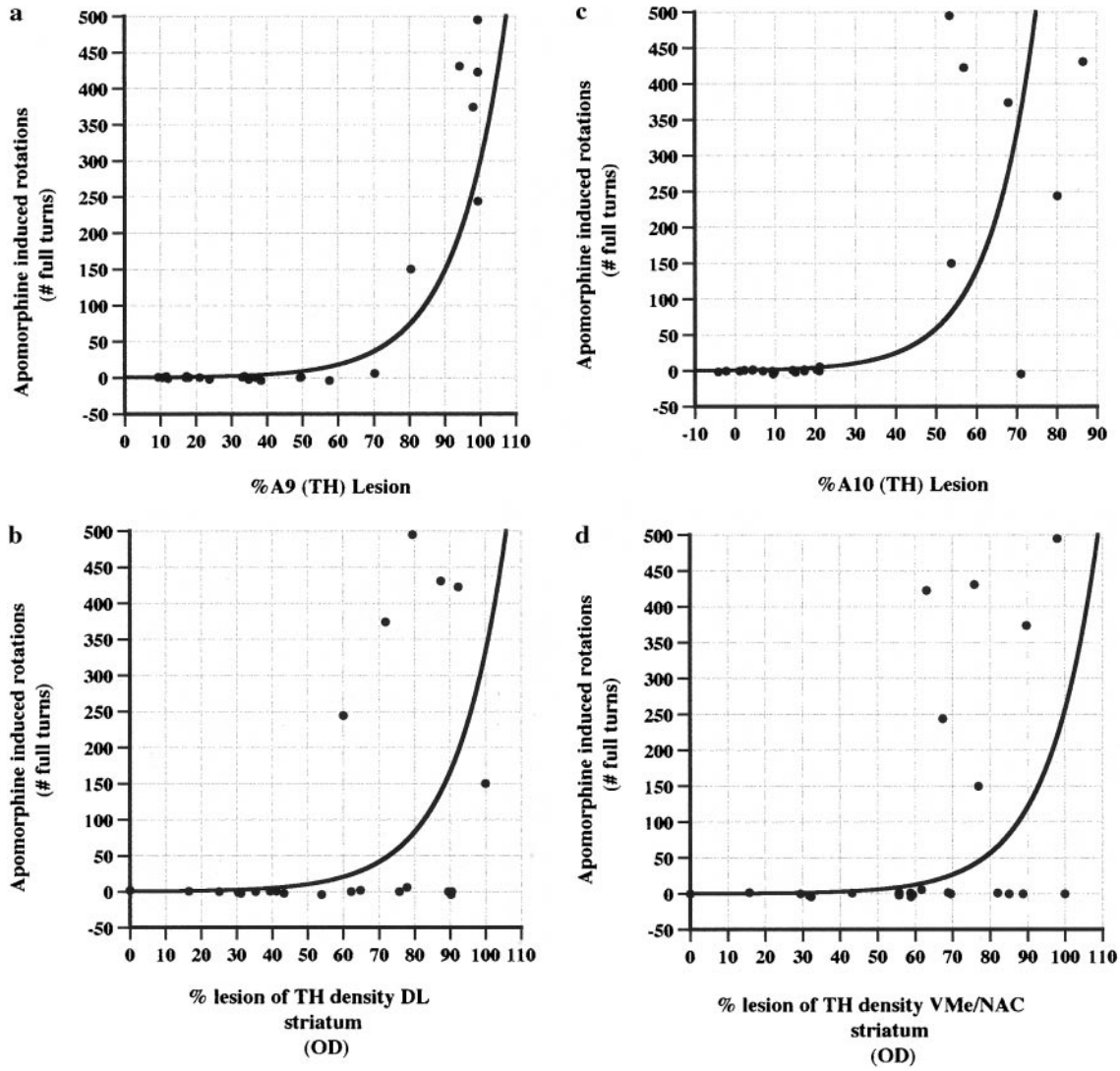


**FIG. 5.** Correlations between the number of apomorphine-induced rotations (number of full turns) and the percentage of lesion of A9 TH-positive cells and A10 TH-positive cells compared to the contralateral side. In addition, percentage loss of TH-positive fibers in the DL and VMe/NAC striatum [measured in optical density (OD) units] and turning were correlated. (a) The model that best fit the correlation between the number of apomorphine-induced rotations and the extent of TH-positive neuronal loss in A9 was a semilogarithmic fit: $\ln(y) = 0.051x + 0.221$, $R^2 = 0.69$, $F$ statistic (df = 1,22) of 55.5, $P < 0.0001$. (b) Correlation between the number of apomorphine-induced rotations and the extent of lesion to $TH^+$ fibers in the DL striatum did not reach significance, however, following a strong exponential trend similar to that seen for the A9 DA neuronal lesions. (c) The model that best described the correlation between the number of apomorphine-induced rotations and the extent of additional A10 TH-positive neuronal loss was a semilogarithmic fit: $\ln(y) = 4.60x - 28.7$, $R^2 = 0.55$, $F$ statistic (df = 1, 22) of 33.4, $P < 0.0001$. (d) Correlation between the percentage of lesion to TH-positive fibers in the VMe/NAC striatum and number of apomorphine-induced rotations did not reach significance, however, following a strong exponential trend similar to that seen for the additional A10 neuronal loss.

the extent of A10 lesion, a strong positive linear regression model was also found: $y = 0.96x - 8.30$. This model was statistically significant ($R^2 = 0.43$), with an overall $F$ statistic (df = 1,22) of 16.3 ($P = 0.0005$). These data (Fig. 7c) suggest that ipsilateral side bias increases linearly throughout the entire measured range (0–100%) of additional A10 DA lesion.

*Total head-turning activity.* When we analyzed the total number of head turns made and correlated these data with both A9 cell loss and DL striatal $TH^+$ fiber density, no significant correlations were found. However, $TH^+$ fiber density of the VMe/NAC striatum correlated with the total number of head turns made. The best-fitting model was linear: $y = 0.45x + 50.5$, with $R^2 = 0.18$ and an overall $F$ statistic (df = 1,22) of 4.93 ($P < 0.037$).

*Paw reaching.* Preliminary analysis of these data showed two rats to be consistent nonperformers during the whole 10 days of testing. Subsequent modeling analysis excluded these two nonperformers. Skilled paw-reaching activity was found to be diminished as a function of lesion extent only in the contralateral paw.

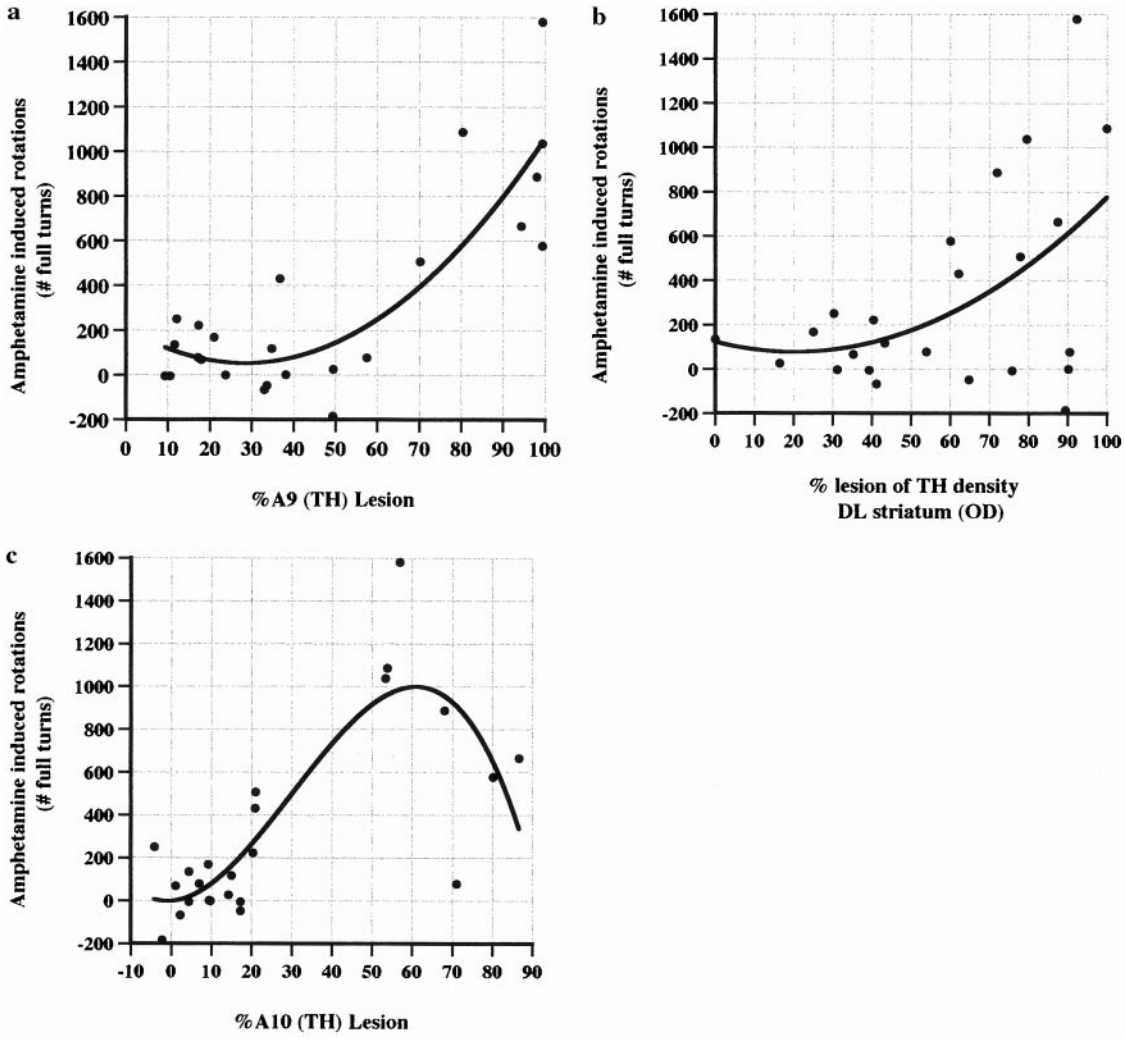


**FIG. 6.** Correlations between the number of amphetamine-induced rotations (number of full turns) and the percentage of lesion of A9 TH-positive cells and A10 TH-positive cells compared to the contralateral side. In addition, the percentage loss of TH-positive fiber density in the DL striatum (measured in OD units) was correlated with turning. (a) The model that best fit the correlation between the number of amphetamine-induced rotations and the extent of TH-positive neuronal lesion in A9 was a second-order polynomial: $y = -11.1x + 0.20x^2 = 208.7$, $R^2 = 0.73$, $F$ statistic (df = 2, 21) of 28.4, $P < 0.0001$. (b) The model that best fit the correlation between the number of amphetamine-induced rotations and the extent of lesion to TH-positive fibers in the DL striatum was a second-order polynomial: $y = 3.27x + 1.32x^2 + 79.3$, $R^2 = 0.25$, $F$ statistic (df = 2,21) of 3.58 ($P = 0.04$). (c) The model that best fit the correlation between the number of amphetamine-induced rotations and the extent of additional A10 TH-positive neuronal loss was a cubic polynomial: $y = 1.32x + 0.77x^2 - 0.008x^3 - 2.40$, $R^2 = 0.67$, $F$ statistic (df = 3, 20) of 13.38, $P < 0.0001$.

For this paw, the typical data pattern was ⌝-shaped, with little or no effect on paw-reaching accuracy at low levels of lesion percentage, a flat relationship until a certain threshold value of lesion extent was reached, and then a rapid falloff of paw-reaching accuracy at high levels of lesion extent. Within the A9 DA lesion data, the model best describing the correlation between the accuracy of left paw reaching and the extent of A9 DA lesion was quadratic: $y = -0.003x^2 - 0.005x + 61.0$. This quadratic regression was statistically significant ($R^2 = 0.26$), with an overall $F$ statistic (df = 2,19) of 3.31 ($P < 0.05$) (Fig. 8a). For DL striatal density, no correlation with paw reaching was found. In a pattern very similar to that of the A9 lesions, additional A10 DA lesion extent was strongly negatively correlated with accuracy of left paw reaching. The best-fitting model was quadratic: $y = -0.011x^2 + 0.33x + 58.9$. This correlation was statistically significant ($R^2 = 0.51$), with an overall $F$ statistic (df = 2,19) of 10.1 ($P < 0.001$). This scatterplot (Fig. 8b) suggests that skilled paw reaching in the contralateral paw is effected only after 30–40% additional A10 DA lesion.

The best-fitting model associating the total number of pellets eaten with the left paw and the extent of A9 DA lesion was quadratic: $y = -0.02x^2 + 1.77x + 53.5$. This correlation was statistically significant ($R^2 = 0.29$), with an overall $F$ statistic (df = 2,19) of 3.95 ($P = 0.037$). This equation suggests that A9 DA

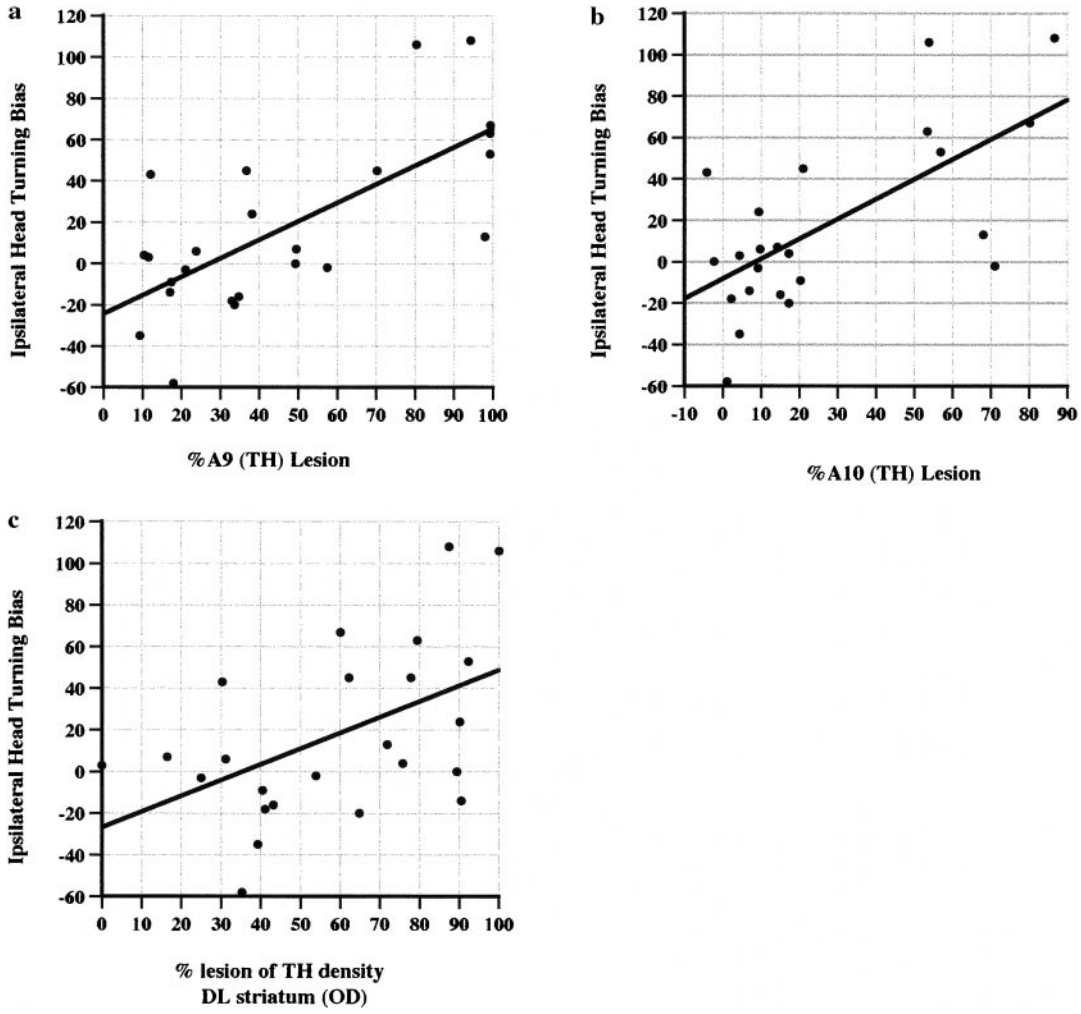


**FIG. 7.** Correlations between the ipsilateral head-turning bias and percentage loss of A9 TH-positive cells and A10 TH-positive cells. In addition, TH-positive fiber density loss in the DL striatum (measured in OD units) was correlated with ipsilateral head-turning bias. (a) The model that best fit the correlation between the ipsilateral head-turning bias and the extent of A9 TH-positive neuronal lesion was a linear fit: $y = 0.90x - 24.5$, $R^2 = 0.50$, $F$ statistic (df = 1, 22) of 21.9, $P < 0.0001$. (b) The model that best fit the correlation between the ipsilateral head-turning bias and TH-positive fiber loss in the DL striatum was a linear fit: $y = 0.75x - 26.7$, $R^2 = 0.25$, $F$ statistic (df = 1, 22) of 7.44 ($P < 0.012$). (c) The model that best fit the correlation between the number of ipsilateral head turns and the extent of additional A10 TH-positive neuronal lesion was a linear fit: $y = 0.96x - 8.30$, $Rsup2 = 0.43$, $F$ statistic (df = 1, 22) of 16.3, $P = 0.0005$.

lesion of 50–60% is required before loss of skilled motor ability in the contralateral paw is observed, after which skilled motor deficits become more pronounced as lesion approaches 100%. For DL striatal density, no correlation with number of pellets eaten was found. Correlation between the total number of pellets eaten with the left paw and extent of additional A10 DA cell loss yielded a best-fitting quadratic model: $y = -0.02x^2 + 0.43x + 82.8$. This model was statistically significant ($R^2 = 0.41$), with an overall $F$ statistic (df = 2,19) of 6.53 ($P = 0.0069$). The data pattern suggests that additional A10 DA lesion is associated with loss in skilled paw-reaching ability that intensifies after approximately 20–30% A10 DA lesion. For DL striatal density, no correlation with number of pellets eaten was found.

## DISCUSSION

In this experiment we have demonstrated that A9 (SNc) DA degeneration increased amphetamine rotational motor behavior in a linear manner above approximately 40–50% DA cell loss, while additional DA cell loss above 60% in the A10/VTA produced a progressive decline (cubic polynomial) in such amphetamine-induced rotation. We have also shown that spontaneous ipsilateral side bias in head turning increased with the degree of SNc and VTA DA neuron loss and DL striatal DA as assessed by DA ($TH^+$) fiber density loss, while the total head-turning activity increased with DA ($TH^+$) fiber density loss in striatal regions innervated by the A10/VTA.

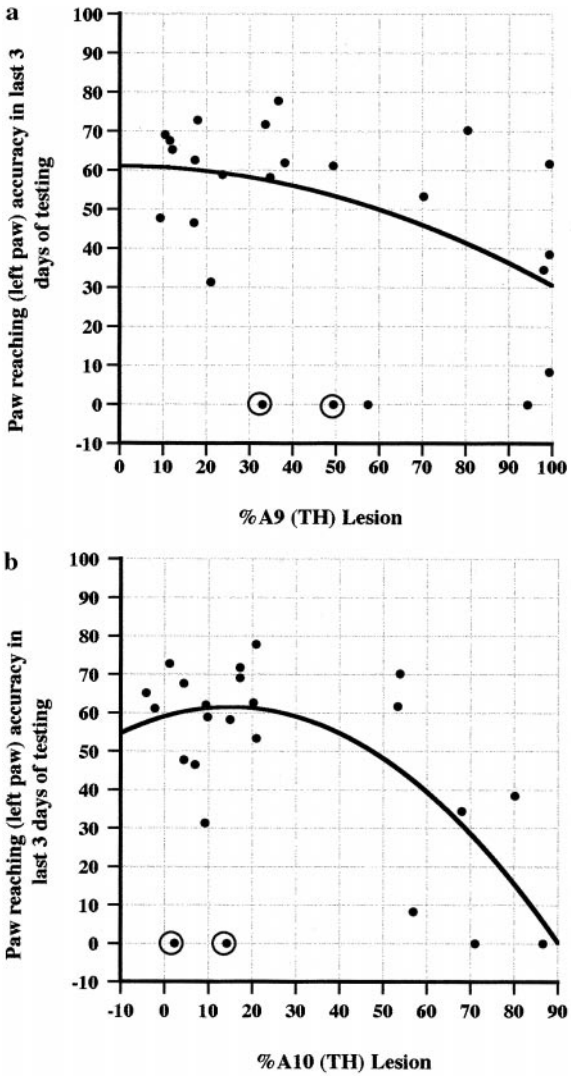


**FIG. 8.** Correlations were made between the average accuracy of the left paw over the last 3 days of testing and the percentage of lesion to the A9 TH-positive cells and A10 TH-positive cells. In addition, correlations between the total number of pellets eaten with the left paw during the whole 10 days of paw-reaching tests and the percentage of lesion to A9 TH-positive cells and A10 TH-positive cells were made. Analysis of these data showed two rats to be consistent nonperformers (circled points) during the whole 10 days of testing. Subsequent modeling analyses excluded these rats. (a) The model that best fit the correlation between the average accuracy of the left paw during the last 3 days of testing and the extent of the A9 TH-positive neuronal lesion was a quadratic fit: $y = 0.003x^2 - 0.005x + 61.0$, $R^2 = 0.26$, $F$ statistic (df = 2, 19) of 3.31 ($P < 0.05$). (b) The model that best fit the correlation between the average accuracy of the left paw during the last 3 days of testing and the extent of the additional A10 TH-positive neuronal lesion was a quadratic fit: $y = -0.011x^2 + 0.33x + 58.9$, $R^2 = 0.51$, $F$ statistic (df = 2, 19) of 10.1, $P < 0.001$.

### *Drug-Induced Behavioral Responses*

*Apomorphine-induced rotation.* An exponential model describing the supersensitivity effect of apomorphine as a full DA agonist on turning behavior suggested that contralateral rotations are not induced until A9 DA lesions of approximately 70–80% are attained. At this point the number of rotations made during the test increases with A9 DA lesion. This is supported by previous research indicating that apomorphine-induced rotations are not apparent until greater cell loss is achieved (23, 32, 44).

The model best describing the effect of additional A10 DA lesion was also exponential and indicated that the rate of contralateral rotation increases with the extent of additional A10 DA lesion, after a threshold lesion of 70–80% is achieved. Based on the strength of the model describing the effect of A9 cell loss on apomorphine rotations and previous studies involving the nigrostriatal DA system (23, 44), which also show the presence of this threshold, it is likely that the exponential fit is a fair representation of the physiological system. Although neither DL striatal density nor VMe/NAC striatum $TH^+$ fiber density correlated with the number of contralateral rotations observed producing significant correlations, strong exponential trends support the existence of the threshold, suggesting that contralateral rotational behavior is not observed until $TH^+$ fiber loss reaches 80–90% in the striatum.

*Amphetamine-induced rotation.* Animals with greater than 50% lesion to the A9 DA neurons start to turn ipsilaterally in response to monoamine (primarily DA) release by amphetamine. Amphetamine-induced rotations are not further effected until an additional A10 DA neuronal loss reaches greater than 60%, at which point rotational behavior diminishes. Although the role of the mesolimbic DA system has not been studied to the same extent as the nigrostriatal DA system in this particular paradigm, research indicates that the A10 DA nucleus does have an effect on A9 DA-mediated behavior (7, 26, 27, 41, 44, 48). Classically, Kelly *et al.* (27) demonstrated that bilateral injection of 6-OHDA into the NAC blocks ipsilateral rotation of unilaterally mfb-lesioned rats, whereas apomorphine-induced rotations were enhanced. It appears that mesolimbic DA excitation, produced by either indirectly or directly acting agonists, has a regulatory effect on the rate of rotation without influencing direction.

*Role for the DA A10 nucleus.* These data are consistent with the idea that the DL striatum contributes to the left/right side bias, whereas the A10 DA system (NAC, VMe, cortex layer VI) has an amplifier function on motor and motivational aspects of behavior. Lesion of either the nigrostriatal or mesolimbic DA pathway causes marked loss of DA in corresponding striatal areas. In the normal brain there is neither uneven distribution of DA nor unilateral supersensitivity of DA receptors; therefore, apomorphine and amphetamine affect both left and right hemispheres equally causing no rotational behavior. According to these data, A9 DA lesion of 40–60% does not cause apomorphine-induced rotations, whereas a significant number of amphetamine rotations are observed, which can be

explained by the fact that such a degree of DA lesion of A9 is not sufficient to induce DL striatum receptor supersensitivity. Apomorphine has direct receptor agonist activity (3, 31) and as receptor supersensitivity has not developed when only 40–60% of the A9 system is lesioned (8, 19, 39, 45, 47), apomorphine takes action on both sides of the brain evenly, resulting in no induced rotations.

According to these data, when A9 DA lesion reaches >60%, apomorphine-induced rotations are observed, whereas the rate of amphetamine-induced rotation reaches its climax. This is explained by receptor supersensitivity; when A9 DA lesions are >80%, apomorphine administration causes DA upregulation in the DL striatum causing rotations in a direction contralateral to the lesion (8, 39, 45, 47, 50). A10 amplifies rotational behavior, resulting in the robust induction of rotation rate seen at approximately 80% A9 DA lesion. As A9 DA lesion exceeds 60%, amphetamine administration causes a progressively larger imbalance in DA distribution across left and right hemispheres. A10 acts to enhance rotational behavior; the maximum rate of rotation is attained at 100% A9 DA lesion. Additional A10 DA lesion of 40–60% has no further effect on either apomorphine- or amphetamine-induced rotation. Although receptor supersensitivity in the DL striatum has been achieved, none is seen in the VMe/NAC striatum. These data suggest that additional lesion of more than 60–70% of A10 causes an increase in apomorphine-induced rotations; conversely, amphetamine-induced rotational behavior is diminished. Lesions including more than 60–70% of A10 cause receptor upregulation in the VMe/NAC striatum of the lesioned side following low doses of DA agonists (25). Apomorphine administration causes both A9 and A10 DA nuclei to be highly stimulated, leading to greater amplification of the side bias, explaining the peak in contralateral rotational behavior. Reduction or dampening of amphetamine-induced rotational behavior can be accounted for as both A9 and A10 projections are fully degenerated or highly dysfunctional.

### *Spontaneous Behavioral Tests*

*Head-turning test.* This study also examined the use of a head-turning test, a novel non-drug-induced test utilized as a means for determining both ipsilateral side bias and overall activity levels of 6-OHDA-lesioned rats. Ipsilateral head-turning bias as measured by the head-turning test was first described in marmosets during analysis of amphetamine-induced behavioral responses (42). More recently, ipsilateral orientation asymmetries have been described on the basis of head-turning data in the unilaterally mfb-lesioned rat (20). Previously designed to determine the effect of subthalamic nucleus lesion in primate models of PD, the head-turning test aims to determine subtle changes in the rat's sensorimotor behavior, spontaneous side bias, and overall activity levels (4, 5, 20, 21). In this data set, spontaneous head turning showed that as A9 DA lesion increases so does side bias. This was demonstrated by powerful linear models describing how both A9 DA lesion and A9 plus A10 DA lesion effect side bias as measured by head turning. The gradients of these two models were very similar, indicating that additional A10 DA degeneration had little further effect on head-turning behavior. The extent of DL striatal lesion also yielded a positive linear correlation, supporting the idea that spontaneous ipsilateral side bias is mainly A9 mediated. Correlation of A9 DA neuronal lesion and DL striatal $TH^+$ fiber density with total head-turning activity did not yield any significance, whereas significance was reached when percentage lesion of VMe/NAC striatum $TH^+$ fiber density was correlated with overall head-turning activity, producing a positive linear correlation. This suggests that additional A10 DA lesion causes increased levels of activity. As correlation between A9 DA lesion and total head-turning behavior did not reach significance, it is likely that this increase in head-turning activity is caused by additional A10 DA lesion in this spontaneous behavioral paradigm. From this experiment, it is not clear if the hyperactivity effect is dependent upon lesion of A9 and A10 or if it is merely an A10 phenomenon. Research into the effects of chemical stimulation of the mesolimbic DA system indicates that hyperactivity is primarily an A10 DA-mediated behavioral response (15, 22, 24, 30, 33, 40). Bilateral injection of DA, but not of noradrenaline or serotonin, into the NAC of naive rats resulted in stimulation of locomotor activity. In this data set, A10 alone appears to mediate the increase in head-turning activity. This provides further evidence for the idea that A10 plays a role in amplification of A9 DA-mediated behavior.

### *Paw Reaching*

Considering both the average accuracy and the total amount of pellets eaten, quadratic correlations were found to best describe the effect of A9 and A10 DA lesion on skilled motor behavior. Both experiments yielded quadratic models indicating that a threshold lesion of about 40% is required before skilled motor deficits are observed. Unilateral A9 DA lesions greater than about 40% caused skilled motor deficits in the contralateral paw, which intensified as lesion became inclusive of 100% of the SNc DA population. This confirmed previous research suggesting that A9 DA lesion causes a decrease in skilled motor activity (14, 29, 34). Additional A10 DA lesion further intensified this effect, producing more powerful quadratic models suggesting that lesion of the A10 DA nucleus >30–40% causes further skilled motor deficits. This could be explained by the fact that A10 DA neurons have been implicated in behaviors involved in feeding habits, food storage, and motivation (33, 36, 37, 51). Papp *et al.* (36,

37) described how bilateral lesion of A10 DA nuclei can result in the loss of response to hunger and thirst stimuli. This implies that although A9 DA lesion causes impairments in skilled motor deficits, it is likely that loss of additional A10 neurons causes changes in motivation, explaining the further loss of paw-reaching ability observed when lesions include A10 DA neurons.

## CONCLUSIONS

These data are consistent with the idea that the DL striatum contributes to the left/right side bias, whereas the A10 DA system, reaching the regions of the NAC, VMe striatum, and cortex layer VI, has an amplifier function on motor and motivational behavior. Furthermore, the analysis provides a set of statistical and quantitative models of both drug-induced and spontaneous behavioral tests used to identify the extent and specificity of A9/A10 DA lesions.

## ACKNOWLEDGMENTS

This work was supported by the American Parkinson's Disease Foundation (APDA) (A.M.); the NINDS Udall Parkinson's Disease Research Center of Excellence (NS-39793) (O.I.); the Century Foundation, Sarasota Memorial Hospital (O.I.); and the Medical Research Council of Canada (F.C.).

## REFERENCES

1. Abercrombie, M. 1946. Estimation of nuclear population from microtome sections. *Anat. Rec.* **94:** 239–247.
2. Anden, N. E., A. Dahlstrom, K. Fuxe, and K. Larsson. 1966. Functional role of the nigro-neostriatal dopamine neurons. *Acta Pharmacol. Toxicol. (Copenhagen)* **24:** 263–274.
3. Anden, N. E., A. Rubenson, K. Fuxe, and T. Hokfelt. 1967. Evidence for dopamine receptor stimulation by apomorphine. *J. Pharm. Pharmacol.* **19:** 627–629.
4. Annett, L. E., F. L. Martel, D. C. Rogers, R. M. Ridley, H. F. Baker, and S. B. Dunnett. 1994. Behavioral assessment of the effects of embryonic nigral grafts in marmosets with unilateral 6-OHDA lesions of the nigrostriatal pathway. *Exp. Neurol.* **125:** 228–246.
5. Annett, L. E., D. C. Rogers, T. D. Hernandez, and S. B. Dunnett. 1992. Behavioural analysis of unilateral monoamine depletion in the marmoset. *Brain* **115:** 825–856.
6. Bradbury, A. J., B. Costall, A. M. Domeney, P. J. Jenner, C. D. Marsden, and R. J. Naylor. 1986. The neurotoxic actions of 6-hydroxydopamine infused into the rat substantia nigra. *Neurosci. Lett.* **67:** 208–212.
7. Brundin, P., R. E. Strecker, E. Londos, and A. Bjorklund. 1987. Dopamine neurons grafted unilaterally to the nucleus accumbens affect drug-induced circling and locomotion. *Exp. Brain Res.* **69:** 183–294.
8. Buonamici, M., C. Caccia, M. Carpentieri, L. Pegrassi, A. C. Rossi, and G. Di Chiara. 1986. D-1 receptor supersensitivity in the rat striatum after unilateral 6- hydroxydopamine lesions. *Eur. J. Pharmacol.* **126:** 347–348.
9. Buonamici, M., M. A. Cervini, A. C. Rossi, L. Sebastiani, A. Raffaelli, and P. Bagnoli. 1990. Injections of 6-hydroxydopamine in the substantia nigra of the rat brain: Morphological and biochemical effects. *Behav. Brain Res.* **38:** 83–95.
10. Costall, B., C. D. Marsden, R. J. Naylor, and C. J. Pycock. 1976. The relationship between striatal and mesolimbic dopamine dysfunction and the nature of circling responses following 6-hydroxydopamine and electrolytic lesions of the ascending dopamine systems of rat brain. *Brain Res.* **118:** 87–113.
11. Costantini, L. C., P. Chaturvedi, D. M. Armistead, P. G. McCaffrey, T. W. Deacon, and O. Isacson 1998. A novel immunophilin ligand: Distinct branching effects on dopaminergic neurons in culture and neurotrophic actions after oral administration in an animal model of Parkinson's disease. *Neurobiol. Dis.* **5:** 97–106.
12. Costantini, L. C., S. C. Feinstein, M. J. Radeke, and A. Snyder-Keller. 1999. Compartmental expression of trkB receptor protein in the developing striatum. *Neuroscience* **89:** 505–513.
13. Costantini, L. C., and O. Isacson. 2000. Immunophilin ligands and GDNF enhance neurite branching or elongation from developing dopamine neurons in culture. *Exp. Neurol.* **164:** 60–70.
14. Dunnett, S. B., O. Isacson, D. J. Sirinathsinghji, D. J. Clarke, and A. Bjorklund. 1988. Striatal grafts in rats with unilateral neostriatal lesions—III. Recovery from dopamine-dependent motor asymmetry and deficits in skilled paw reaching. *Neuroscience* **24:** 813–820.
15. Galey, D., H. Simon, and M. Le Moal. 1977. Behavioral effects of lesions in the A10 dopaminergic area of the rat. *Brain Res.* **124:** 83–97.
16. Galpern, W. R., L. H. Burns, T. W. Deacon, J. Dinsmore, and O. Isacson. 1996. Xenotransplantation of porcine fetal ventral mesencephalon in a rat model of Parkinson's disease: Functional recovery and graft morphology. *Exp. Neurol.* **140:** 1–13.
17. Garcia, A. R., T. W. Deacon, J. Dinsmore, and O. Isacson. 1995. Extensive axonal and glial fiber growth from fetal porcine cortical xenografts in the adult rat cortex. *Cell Transplant.* **4:** 515–527.
18. Glinka, Y., M. Gassen, and M. B. Youdim. 1997. Mechanism of 6-hydroxydopamine neurotoxicity. *J. Neural Transm. Suppl.* **50:** 55–66.
19. Hefti, F., E. Melamed, and R. J. Wurtman. 1980. Partial lesions of the dopaminergic nigrostriatal system in rat brain: Biochemical characterization. *Brain Res.* **195:** 123–137.
20. Henderson, J. M., L. E. Annett, L. J. Ryan, , W. Chiang, S. Hidaka, E. M. Torres, and S. B. Dunnett. 1999. Subthalamic nucleus lesions induce deficits as well as benefits in the hemiparkinsonian rat. *Eur. J. Neurosci.* **11:** 2749–2757.
21. Henderson, J. M., L. E. Annett, E. M. Torres, and S. B. Dunnett. 1998. Behavioural effects of subthalamic nucleus lesions in the hemiparkinsonian marmoset (*Callithrix jacchus*). *Eur. J. Neurosci.* **10:** 689–698.
22. Herman, J. P., K. Choulli, N. Abrous, J. Dulluc, and M. Le Moal. 1988. Effects of intra-accumbens dopaminergic grafts on behavioral deficits induced by 6-OHDA lesions of the nucleus accumbens or A10 dopaminergic neurons: A comparison. *Behav. Brain Res.* **29:** 73–83.
23. Hudson, J. L., C. G. van Horne, I. Stromberg, S. Brock, J. Clayton, J. Masserano, B. J. Hoffer, and G. A. Gerhardt. 1993. Correlation of apomorphine- and amphetamine-induced turning with nigrostriatal dopamine content in unilateral 6-hydroxydopamine lesioned rats. *Brain Res.* **626:** 167–174.
24. Joyce, E. M., and S. D. Iversen. 1979. The effect of morphine applied locally to mesencephalic dopamine cell bodies on spontaneous motor activity in the rat. *Neurosci. Lett.* **14:** 207–212.
25. Joyce, E. M., L. Stinus, and S. D. Iversen. 1983. Effect of injections of 6-OHDA into either nucleus accumbens septi or frontal cortex on spontaneous and drug-induced activity. *Neuropharmacology* **22:** 1141–1145.

26. Kelly, P. H., and K. E. Moore. 1976. Mesolimbic dopaminergic neurones in the rotational model of nigrostriatal function. *Nature* **263:** 695–696.
27. Kelly, P. H., and K. E. Moore. 1977. Mesolimbic dopamine neurons: Effects of 6-hydroxydopamine-induced destruction and receptor blockade on drug-induced rotation of rats. *Psychopharmacology (Berlin)* **55:** 35–41.
28. Kelly, P. H., P. W. Seviour, and S. D. Iversen. 1975. Amphetamine and apomorphine responses in the rat following 6-OHDA lesions of the nucleus accumbens septi and corpus striatum. *Brain Res.* **94:** 507–522.
29. Kirik, D., C. Rosenblad, and A. Bjorklund. 1998. Characterization of behavioral and neurodegenerative changes following partial lesions of the nigrostriatal dopamine system induced by intrastriatal 6-hydroxydopamine in the rat. *Exp. Neurol.* **152:** 259–277.
30. Koob, G. F., L. Stinus, and M. Le Moal. 1981. Hyperactivity and hypoactivity produced by lesions to the mesolimbic dopamine system. *Behav. Brain Res.* **3:** 341–359.
31. LaHoste, G. J., and J. F. Marshall. 1990. Nigral D1 and striatal D2 receptors mediate the behavioral effects of dopamine agonists. *Behav. Brain Res.* **38:** 233–242.
32. Lee, C. S., H. Sauer, and A. Bjorklund. 1996. Dopaminergic neuronal degeneration and motor impairments following axon terminal lesion by intrastriatal 6-hydroxydopamine in the rat. *Neuroscience* **72:** 641–653.
33. Mogenson, G. J., D. L. Jones, and C. Y. Yim. 1980. From motivation to action: Functional interface between the limbic system and the motor system. *Prog. Neurobiol.* **14:** 69–97.
34. Montoya, C. P., L. J. Campbell-Hope, K. D. Pemberton, and S. B. Dunnett. 1991. The "staircase test": A measure of independent forelimb reaching and grasping abilities in rats. *J. Neurosci. Methods* **36:** 219–228.
35. Moore, A. E., F. Ciccetti, L. Bjorklund, and O. Isacson. 2000. Comparative motor test methodologies in the 6-OHDA rat model of Parkinson's disease. 27th Annual Society for Neuroscience, New Orleans.
36. Papp, M., and A. Bal. 1986. Motivational versus motor impairment after haloperidol injection or 6-OHDA lesions in the ventral tegmental area or substantia nigra in rats. *Physiol. Behav.* **38:** 773–779.
37. Papp, M., and A. Bal. 1987. Separation of the motivational and motor consequences of 6-hydroxydopamine lesions of the mesolimbic or nigrostriatal system in rats. *Behav. Brain Res.* **23:** 221–229.
38. Paxinos, G., and C. Watson. 1986. *The Rat Brain in Stereotaxic Co-ordinates,* 2nd ed. Academic Press, San Diego.
39. Piccini, P., D. J. Brooks, A. Bjorklund, R. N. Gunn, P. M. Grasby, O. Rimoldi, P. Brundin, P. Hagell, S. Rehncrona, H. Widner, and O. Lindvall. 1999. Dopamine release from nigral transplants visualized *in vivo* in a Parkinson's patient [see comments]. *Nat. Neurosci.* **2:** 1137–1140.
40. Pijnenburg, A. J., W. M., Honig, J. A. Van der Heyden, and J. M. Van Rossum. 1976. Effects of chemical stimulation of the mesolimbic dopamine system upon locomotor activity. *Eur. J. Pharmacol.* **35:** 45–58.
41. Sakai, K., and D. M. Gash. 1994. Effect of bilateral 6-OHDA lesions of the substantia nigra on locomotor activity in the rat. *Brain Res.* **633:** 144–150.
42. Scraggs, P. R., and R. M. Ridley. 1978. Behavioural effects of amphetamine in a small primate: Relative potencies of the d- and l-isomers. *Psychopharmacology (Berlin)* **59:** 243–245.
43. Thoenen, H., and J. P. Tranzer. 1968. Chemical sympathectomy by selective destruction of adrenergic nerve endings with 6-hydroxydopamine. *Naunyn Schmiedeberg's Arch .Exp. Pathol. Pharmacol.* **261:** 271–288.
44. Thomas, J., J. Wang, H. Takubo, J. Sheng, S. de Jesus, and K. S. Bankiewicz. 1994. A 6-hydroxydopamine-induced selective parkinsonian rat model: Further biochemical and behavioral characterization. *Exp. Neurol.* **126:** 159–167.
45. Thornburg, J. E., and K. E. Moore. 1975. Supersensitivity to dopamine agonists following unilateral, 6-hydroxydopamine-induced striatal lesions in mice. *J. Pharmacol. Exp. Ther.* **192:** 42–49.
46. Ungerstedt, U. 1968. 6-Hydroxy-dopamine induced degeneration of central monoamine neurons. *Eur. J. Pharmacol.* **5:** 107–110.
47. Ungerstedt, U. 1971. Postsynaptic supersensitivity after 6-hydroxy-dopamine induced degeneration of the nigro-striatal dopamine system. *Acta Physiol. Scand. Suppl.* **367:** 69–93.
48. Ungerstedt, U. 1971. Striatal dopamine release after amphetamine or nerve degeneration revealed by rotational behaviour. *Acta Physiol. Scand. Suppl.* **367:** 49–68.
49. Ungerstedt, U., and G. W. Arbuthnott. 1970. Quantitative recording of rotational behavior in rats after 6-hydroxy-dopamine lesions of the nigrostriatal dopamine system. *Brain Res.* **24:** 485–493.
50. Ungerstedt, U., T. Ljungberg, B. Hoffer, and G. Siggins. 1975. Dopaminergic supersensitivity in the striatum. *Adv. Neurol.* **9:** 57–65.
51. Ungerstedt, U., T. Ljungberg, and G. Steg. 1974. Behavioral, physiological, and neurochemical changes after 6- hydroxydopamine-induced degeneration of the nigro-striatal dopamine neurons. *Adv. Neurol.* **5:** 421–426.
52. van Domburg, P. H., and H. J. ten Donkelaar. 1991. The human substantia nigra and ventral tegmental area. A neuroanatomical study with notes on aging and aging diseases. *Adv. Anat. Embryol. Cell Biol.* **121:** 1–132.